Am J Cancer Res 2016;6(6):1271-1286
www.ajcr.us /ISSN:2156-6976/ajcr0031097

Original Article

Synthesis of a novel adamantyl nitroxide derivative with potent anti-hepatoma activity in *vitro* and in *vivo*

Jin Sun[1,3*], Shan Wang[1*], Wei Bu[1], Meng-Ying Wei[2], Wei-Wei Li[1], Min-Na Yao[1], Zhong-Ying Ma[1], Cheng-Tao Lu[1], Hui-Hui Li[3], Na-Ping Hu[3], En-Hu Zhang[3], Guo-Dong Yang[2], Ai-Dong Wen[1], Xiao-He Zhu[1]

[1]Department of Pharmacy, Xijing Hospital, Fourth Military Medical University, Xi'an, Shaanxi 710032, China; [2]State Key Laboratory of Cancer Biology, Department of Biochemistry and Molecular Biology, Fourth Military Medical University, Xi'an, Shaanxi 710032, China; [3]College of Pharmacy, Shaanxi University of Chinese Medicine, Xianyang, Shaanxi 712046, China. [*]Equal contributors.

Received April 22, 2016; Accepted May 16, 2016; Epub June 1, 2016; Published June 15, 2016

Abstract: In this study, a novel adamantyl nitroxide derivative was synthesized and its antitumor activities *in vitro* and *in vivo* were investigated. The adamantyl nitroxide derivative **4** displayed a potent anticancer activity against all the tested human hepatoma cells, especially with IC_{50} of 68.1 μM in Bel-7404 cells, compared to the positive control 5-FU (IC_{50}=607.7 μM). The significant inhibition of cell growth was also observed in xenograft mouse model, with low toxicity. Compound **4** suppressed the cell migration and invasion, induced the G2/M phase arrest. Further mechanistic studies revealed that compound **4** induced cell death, which was accompanied with damaging mitochondria, increasing the generation of intracellular reactive oxygen species, cleavages of caspase-9 and caspase-3, as well as activations of Bax and Bcl-2. These results confirmed that adamantyl nitroxide derivative exhibited selective antitumor activities via mitochondrial apoptosis pathway in Bel-7404 cells, and would be a potential anticancer agent for liver cancer.

Keywords: Adamantyl nitroxide derivative, hepatoma, anticancer, apoptosis, reactive oxygen species

Introduction

Hepatocellular carcinoma (HCC) is one of the most common and deadly human malignancies, accounting for the second leading cause of cancer related death worldwide [1]. Although surgical techniques and chemotherapies for HCC have been improved, the five-year survival rate of HCC is still significantly lower than other cancer types [2-4]. Currently, there are several problems associated with current anti-hepatoma drugs, including poor efficacy, drug resistance and toxic side effects [5]. Further development of new anti-hepatoma drugs with high efficiency and low toxicity is still urgently required.

Nitroxide radicals are stable free radicals that have unique antioxidant properties and promote the metabolism of many reactive oxygen species (ROS). They possess a wide range of bioactivities, such as radioprotective effect [6], anti-inflammatory [7], neuroprotective effect [8], antinociceptive effect [9] and antitumor [10]. Tempol (4-hydroxy-2, 2, 6, 6-tetramethylpiperidine-*N*-oxyl), one of the nitroxide radicals, which is characterized by excellent membrane permeability [11], has been studied intensively. Furthermore, Tempol was considered as a pharmaceutical molecule to modify the lead compounds for improvement of the antitumor activity [12]. For example, it has been reported that introducing of Tempol moiety into triazene derivatives (SLTA6) would improve the selectivity in killing melanoma B16 [13].

Adamantyl group is frequently found in biologically active compounds. Several adamantyl-derived drugs play important roles in current cancer therapy [14]. Incorporation of an adamantyl moiety usually results in increased lipophilicity and thus enhanced biological availability [15]. Besides, the adamantyl group could improve the therapeutic efficacy of lead com-

pounds via a variety of other mechanisms [16]. It has been reported that adamantyl modified (aryloxyacetylamino)benzoic acid represents a novel class of HIF-1 inhibitors, which potently inhibited the HIF-1α protein accumulation in human hepatocellular carcinoma Hep3B cells [17]. In addition, the adamantyl-modified retinoid showed potent proapoptotic and antiangiogenesis activity in solid tumors, with an improved pharmacological profile [18]. Therefore, hybridization of anticancer drugs with adamantyl moiety would be a rational design to improve affinity and efficacy, when compared to the parent drugs [19]. We previously used the attractive strategy to synthesize a series of adamantyl nitroxide derivatives, which were composed of both active pharmacophores of adamantyl moiety and Tempol. The compound exhibited antiproliferative activity against human hepatoma cells [20].

In the current study, a new adamantyl nitroxide derivative is synthesized, namely compound **4**. Its antiproliferative effects on human hepatoma HepG2, SMMC-7721, MHCC-97H, Bel-7404 and human normal L-02 cells are evaluated, and the possible molecular mechanism for its biological activity is also explored in this study.

Materials and methods

Chemicals and instrument

All chemical reagents were purchased from commercial suppliers and used without further purification. Melting points were determined on X-6 melting point apparatus and were uncorrected. IR was recorded as thin films on KBr plates with BRUKER TENSOR 27 spectrophotometer. Electrospray ionization mass spectra (ESI-MS) analysis was carried out on Agilent 6410 mass spectrometer. Elemental analyses were measured on Elementar VarioEL III apparatus.

Cells and animals

Human hepatoma Bel-7404, HepG2, SMMC-7721, MHCC-97H and human normal liver L-02 were obtained from the State Key Laboratory of Cancer Biology, Fourth Military Medical University (Xi'an, China). Cells were cultured in PRIM-1640 medium (HyClone), supplemented with 10% FBS and 1% antibiotics (HyClone) (100 IU/mL penicillin and 100 μg/mL streptomycin) at 37°C in a 5% CO_2 atmosphere. Male nude mice (4-6 weeks old, weight: 18-20 g) were purchased from Experiment Animal Center of Fourth Military Medical University. All animal procedures were performed in accordance with the protocols approved by Animal Care and Use Committee of Fourth Military Medical University.

Synthesis of adamantyl nitroxide derivative

Adamantyl nitroxide derivative was prepared according to our previous study [20]. Dissolving 1, 3-adamantanedicarboxylic acid (4.48 g, 20 mmol) in MeOH (50 mL) and H_2SO_4 (0.25 mL) gave crude compound **1** as white powder. Compound **1** was dissolved in THF (25 mL) and a solution of NaOH (0.8 g) in MeOH (8 mL) was added. The reaction mixture was stirred at room temperature overnight. Then the reaction was treated with water and extracted with CH_2Cl_2. The alkaline aqueous extraction was acidified with 6 N HCl until pH=3 and extracted with CH_2Cl_2. Compound **2** was obtained as a white solid.

To a solution of compound **2** and thionyl chloride (3.6 mL, 50 mmol) in THF (20 mL), two drops of *N, N*-dimethylformamide were added. The reaction mixture was refluxed for 3 h and solvents were evaporated. Subsequently the intermediate **3** was added to a stirred solution of Tempol (2.07 g, 12 mmol) and triethylamine (1.6 mL, 12 mmol) in toluene (50 mL). The resulting mixture was stirred for 8 h at 70°C. Column chromatography (petroleum ether/EtOAc) of the crude product gave Compound **4** as an orange solid (**Scheme 1**), with parameters: M.p. 99-101°C; IR (KBr, cm^{-1}): 2970 (C-H), 1726 (C=O), 1461 (N-O), 1097 (C-O); MS (ESI) *m/z* (%): 393.21 $[M+H]^+$; Anal. calc. for $C_{22}H_{34}NO_5$: C, 67.32; H, 8.73; N, 3.57. Found: C, 67.19; H, 8.76; N, 3.59.

MTT cell viability assay

Cell viability was measured by MTT (3-(4, 5-dimethylthiazol-2-yl)-2, 5-diphenyltetrazolium bromide) (MP, USA) colorimetric assay. Briefly, cells were seeded in 96-well plates at the density of 10^4 cells per well. After 24 h of incubation at 37°C in 200 uL medium under 5% CO_2, cells were treated with indicated drugs for another 24 h and 48 h, and then incubated at 37°C with MTT (50 μL, 1 mg/mL) for additional

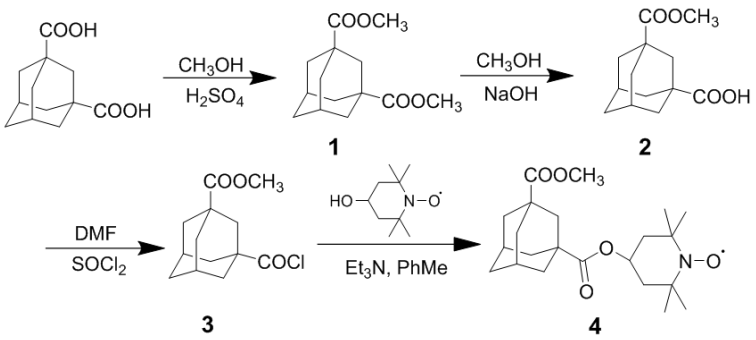

Scheme 1. Synthetic route of adamantyl nitroxide derivative.

4 hours. The absorbance at 490 nm was measured with a MULTISKAN GO microplate reader (THERMO, USA). The antiproliferative activity was presented as the percentage of cell viability reducion. The experiments were performed at least three times.

Examination of the cell cycle distribution and apoptosis by flow cytometry

Cell cycle and apoptosis were analyzed by flow cytometry (BD FACSAria). A total of 10^4 cells were used to analyze the cell cycle distribution with MultiCycle software (USA). For cell cycle analysis, the treated cells were washed twice with PBS, and fixed in pre-cooled alcohol and PBS (2:1) at -20°C overnight. Cells were treated with RNase A (0.05 mg/ml) for 30 min at 37°C, and then were incubated with 10 μL of PI solution (50 μg/mL in 500 μL PBS) for 30 min in the dark. For apoptosis analysis, cells at the logarithmic growth phase were harvested and seeded at 1 × 10^6 cells/mL on 6-well plate. Twenty-four hours after cell seeding, cells were subjected to indicate treatments for additional 24 or 48 h, and then subjected to Annexin V and propidium iodide (PI) staining using an Annexin V-FITC Apoptosis Detection Kit.

Cell migration and invasion assay

Cells were seeded on Transwell insert of the 24-Well Cell Migration and Invasion Assay Kit (BD-Falcon, USA), with the top chamber uncoated and coated respectively. In the bottom chamber, 10% FBS was used as the chemoattractant. The 24-well dish was incubated at 37°C for 24 h. The unmigrated cells on the top chamber were removed. The migrated and invaded cells on the lower membrane surface were stained with Crystal Violet and counted under a microscope (Olympus, Japan).

Transmission electron microscopy (TEM) assay

Cells were fixed in 2.5% glutaraldehyde (pH=7.4) for 48 h, followed by osmium tetroxide. Samples were dehydrated in ethanol, infiltrated and embedded with Epon 812 at 60°C for 24 h, and then sectioned to 70 nm in thickness. Analysis was performed by transmission electron microscopy (× 6000 and × 26500, TECNAI spirit, FEI).

Measurement of intracellular reactive oxygen species (ROS) level

Reactive oxygen species are able to oxidize the cleaved DCFH (2', 7'-dichlorofluorescein diacetate) to DCF, which is highly fluorescent at 530 nm [21]. To measure ROS generation induced by 25, 76, 128 μM of compound **4**, Bel-7404 cells were harvested after 48 h exposure and washed twice with PBS, and then fresh medium containing 10 μM DCFH-DA was added to previously treated cells. For ROS scavenge, Bel-7404 cells were pretreated for 4 h with the 10 mM ROS scavenger (*N*-acetyl-cysteine, NAC) before 48 h of exposure to 128 μM of compound **4**. After 30 min incubation, cells were washed again and observed immediately by flow cytometric assay (BD FACSAria).

Western blot analysis

Western blot was used to detect the expression levels of Bax, Bcl-2, cleaved caspase-9 and caspase-3 proteins in Bel-7404 cells. Immunoblotting was performed as described [22]. Blots were quantitated by densitometry using Image Software (Odyssey, LI-COR, USA) and normalized to a housekeeper marker β-actin.

Bel-7404 xenograft nude mice model

Male nude mice (six-week-old, n=25) were husbanded with sterilized diet and water. Mice were randomly divided into five groups for injection of cancer cells. Bel-7404 cells were harvested for implantation by trypsin and washed

Table 1. Compound **4** inhibited the growth of HCC cells[a]

Compounds	IC_{50} (μM) 48 h (n=3)				
	HepG2	Bel-7404	MHCC-97H	SMMC-7721	L-02
4	81.0±7.2	68.1±5.2	120.8±7.8	131.0±10.3	811.5±9.7
Tempol	6098.2±7.9	3104.5±6.0	5365.7±8.2	1785.5±4.6	27188.0±5.9
5-FU	3669.5±7.5	607.7±7.9	4124.1±11.2	296.2±6.9	1425.1±5.8

[a]Values are expressed as the mean ± standard deviation from 3 independent experiments.

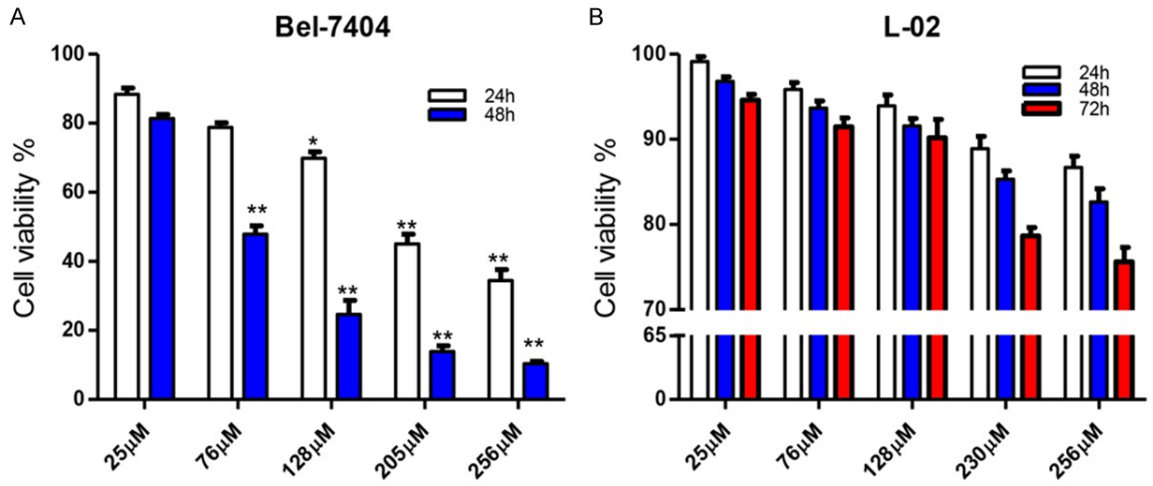

Figure 1. The effect of compound **4** inhibits proliferation in Bel-7404 and L-02 cells. A. The growth-inhibitory effect of various concentrations of compound **4** on Bel-7404 cells for 24 h and 48 h. B. The cytotoxicity of compound **4** on L-02 cells for 24 h, 48 h and 72 h. The data are expressed as the mean ± standard deviation (n=3).

with sterile PBS, followed by suspending in iced-cold PBS and matrigel (1:1) at 5 × 10^7 cells/mL. Bel-7404 cells were injected into the mice subcutaneously at a dose of 1.0 × 10^7/200 μL per mouse. Twenty one days after injection, neoplasm growth was observed macroscopically on the mice. Compound **4** was intraperitoneally injected at one day interval. The vehicle physiologic saline and 1% alcohol was used as control, and 5-FU was used as positive control. Body weights of animals were measured before initiation and during the experiment. Tumor growth was measured every two days over 21 d. Tumor volume (V) was determined by measuring the length (a) and the width (b) and calculated using the equation: $V=(a \times b^2)/2$.

Histopathological analysis

The animals were killed 14 days after compound **4** treatment initiation. The tumor tissues were immediately fixed in 4% neutral buffered formalin at 4°C overnight, then dehydrated and embedded in paraffin. The fixed tissues were divided into two blocks per mice and then processed for paraffin embedding. Tissue sections (5 μm) were cut and stained by hematoxylin and eosin (H&E) for general histological examination.

Terminal deoxynucleotidyl transferase dUTP nick-end labeling (TUNEL) assay

The apoptotic cells in tumor tissue sections were detected using TUNEL assay according to the manufacturer's instructions (Roche, USA). The tissue sections were incubated with Proteinase K for 30 min, and subsequently incubated with the TUNEL reaction mixture that contained terminal deoxynucleotidyl transferase (TdT) and fluorescein-dUTP (1:9) in a humidified chamber for 60 min at 37°C. Slides were rinsed with PBS, and the signal was amplified with horseradish peroxidase-conjugated streptavidin. Sections were counterstained with 4', 6-diamidino-2-phenylindole (DAPI) for 5 min. Cells undergoing apoptosis (green) and nuclei

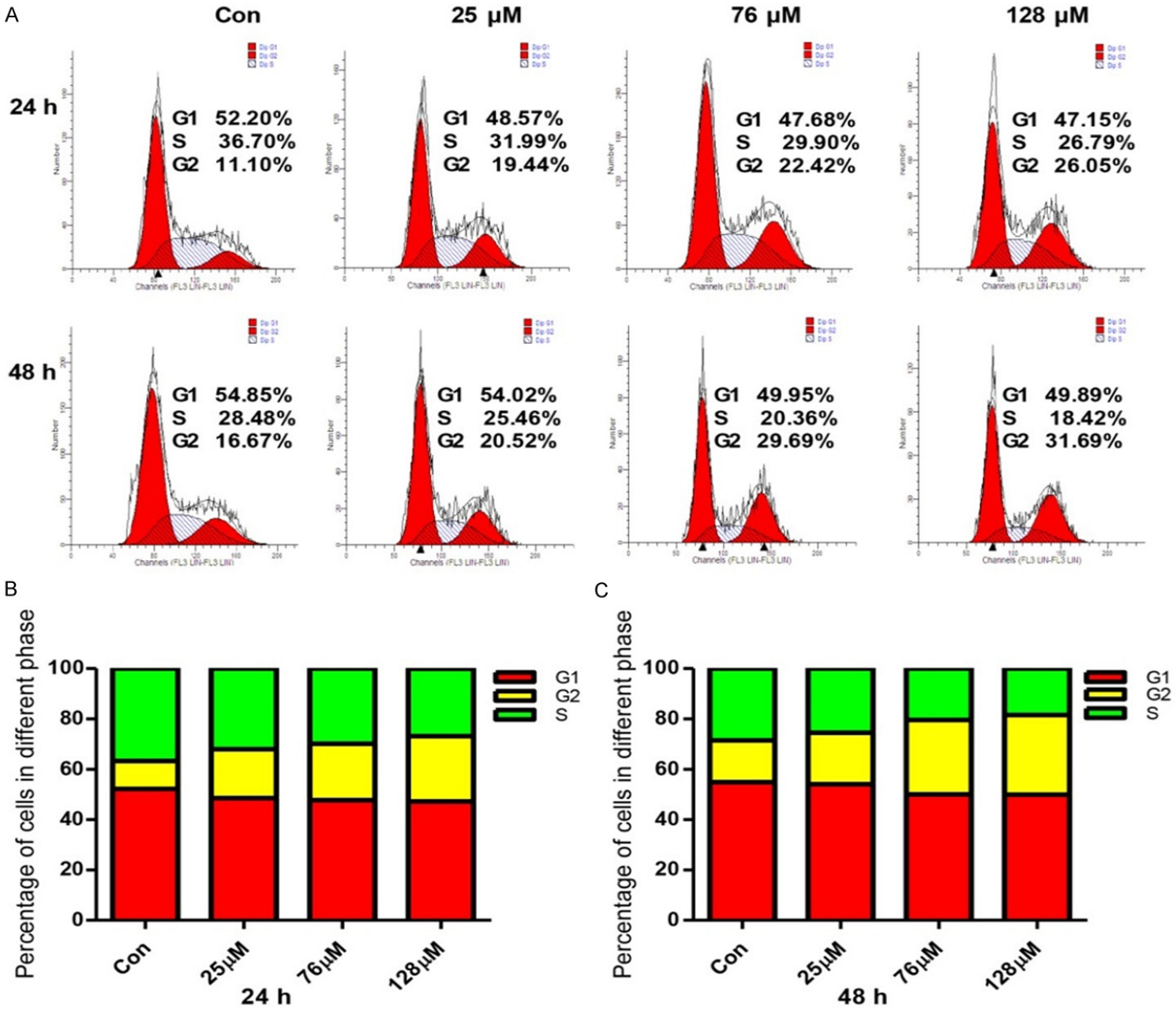
A
Con
25 μM
76 μM
128 μM
24 h
G1 52.20%
S 36.70%
G2 11.10%
G1 48.57%
S 31.99%
G2 19.44%
G1 47.68%
S 29.90%
G2 22.42%
G1 47.15%
S 26.79%
G2 26.05%
48 h
G1 54.85%
S 28.48%
G2 16.67%
G1 54.02%
S 25.46%
G2 20.52%
G1 49.95%
S 20.36%
G2 29.69%
G1 49.89%
S 18.42%
G2 31.69%
B
Percentage of cells in different phase
100
80
60
40
20
0
G1
G2
S
Con
25μM
76μM
128μM
24 h
C
Percentage of cells in different phase
100
80
60
40
20
0
G1
G2
S
Con
25μM
76μM
128μM
48 h

Figure 2. The effects of compound **4** on the cell cycle in Bel-7404 cells. A. Representative images of cells cultured for 24-48 hours from two independent experiments, the results were analyzed with FACS. B, C. Representative results from two independent experiments indicated the percentage of cells in the different phases.

(blue) were examined using a fluorescence microscopy (CK30, Olympus, Japan).

Statistical analysis

The statistical analyses were performed using GraphPad Prism statistical software (GraphPad Software, Inc.). Analysis of variance (ANOVA) or *t*-test was used for comparing the difference between experimental groups. All results were expressed as mean ± standard derivation (SD). The p value of < 0.05 was considered as significant.

Results

*Synthesis and characterization of compound **4***

The adamantyl nitroxide derivative compound **4** was synthesized using the routes outlined in **Scheme 1**. Briefly, dimethyl-adamantane-1, 3-dicarboxylate **1** was prepared starting with 1, 3-adamantanedicarboxylic acid through esterification with methanol. The di-esters **1** was subsequently subjected to mono-hydrolysis with 1 N NaOH in methanol to provide compound **2**, according to literature procedures of Eaton [23]. The compound **4** was derived by the reaction between the acyl chloride intermediate **3** and Tempol, and its structure was characterized and confirmed by IR, ESI-MS and elemental analysis.

*Cell growth inhibition and cytotoxicity of compound **4***

The proliferation and cytotoxicity effects of compound **4** on different HCC cell lines (HepG2, MHCC-97H, SMMC-7721, Bel-7404) and normal L-02 cells were evaluated using MTT assay. Tempol and 5-FU were also included as a bench marker. As shown in **Table 1**, compound **4** exhibited a remarked anticancer activity against all the tested HCC cells with IC_{50} value in a range of concentrations from 68.1 to 131.0 μM. Especially, compound **4** showed stronger inhibitory activity against Bel-7404 cells (IC_{50}= 68.1 μM) than the positive control 5-FU (IC_{50}= 607.7 μM). Compound **4** displayed obvious cell death in a dose- and time-dependent manner on Bel-7404 cells (**Figure 1A**). In contrast, there was no significant cell death in L-02 normal cells after exposure to various concentrations of compound **4** for 24 h or 72 h (**Figure 1B**).

*Compound **4** induces cell cycle arrest and apoptosis*

The effect of compound **4** on cell cycle progression in Bel-7404 cells was determined by flow cytometry. As indicated in **Figure 2A**, there was a significant increase in the proportion of G2/M phase, especially when the concentration of compound **4** was > 76 μM for 48 h (**Figure 2B**, **2C**). Induction of apoptosis is essential for cancer treatment. In the present study, we have also investigated whether the cell death of HCC induced by compound **4** was due to the apoptosis. As expected, compound **4** clearly induced apoptosis in Bel-7404 cells in a dose-dependent manner (**Figure 3A-C**). To investigate the mechanism on the induction of apoptosis, the effects of compound **4** on the expressions of apoptosis-related protein including Bax, Bcl-2, caspase-9 and caspase-3 were detected by western-blot assay, and β-actin was served as the internal standard. As shown in **Figure 3D**, compared to the controls, compound **4** had decreased expression levels of Bcl-2, and markedly increased expression levels of Bax, cleaved caspase-9 and caspase-3 in a dose-dependent manner, further confirming the effects of compound **4** on cell apoptosis.

*Compound **4** reduces migration and invasion*

Migration and invasion are the initial and critical events in metastasis. The effects of compound **4** on cell migration and invasion in Bel-7404 cells were studied using the transwell assay. As expected, compound **4** remarkably decreased migratory capability of Bel-7404 cells (**Figure 4A** and **4C**) in a dose-dependent manner. Similarly, as shown in **Figure 4B** and **4D**, the invasive capability of Bel-7404 cells was also significantly inhibited by high concentration of compound **4** (> 76 μM).

*The effects of compound **4** on cell morphology*

Changes in the morphology of Bel-7404 cells with characteristic apoptotic appearance were

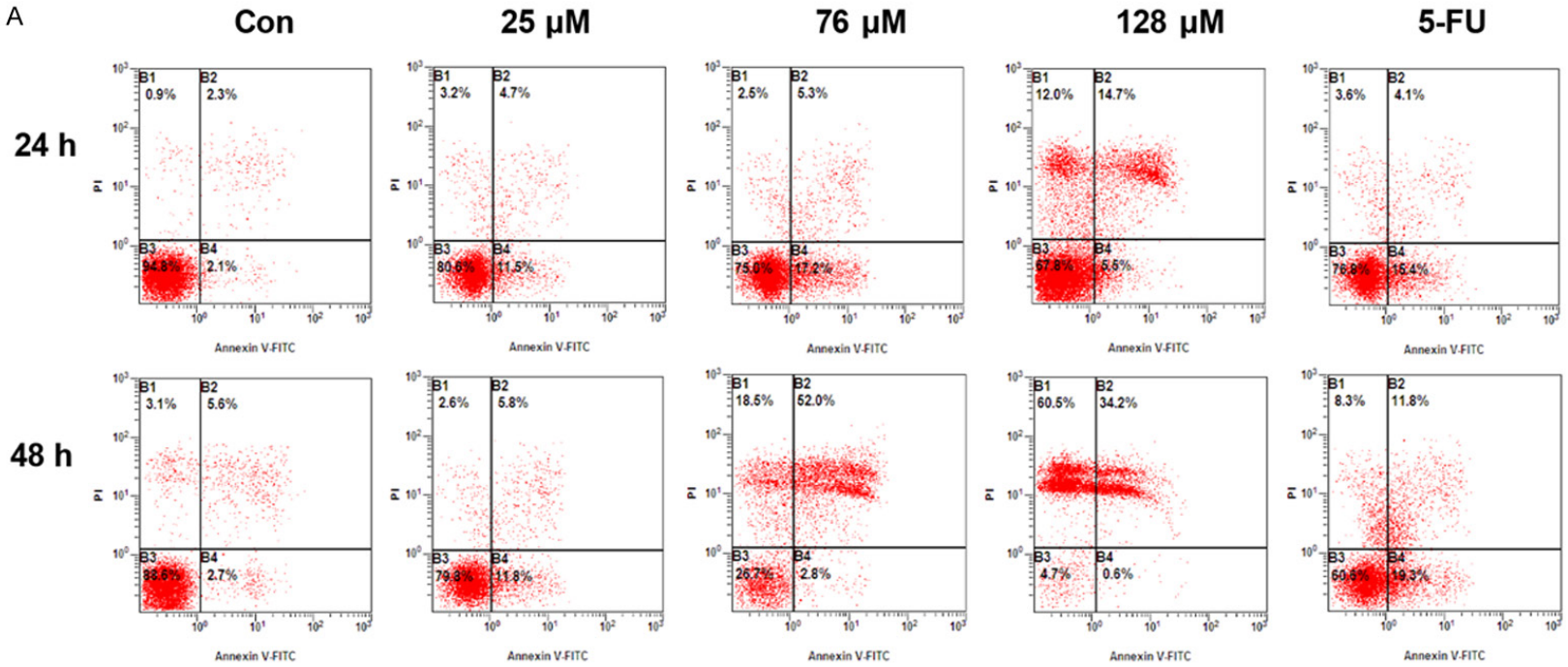
A
Con
25 μM
76 μM
128 μM
5-FU
24 h
48 h
B1 0.9%
B2 2.3%
B3 94.8%
B4 2.1%
B1 3.2%
B2 4.7%
B3 80.6%
B4 11.5%
B1 2.5%
B2 5.3%
B3 75.0%
B4 17.2%
B1 12.0%
B2 14.7%
B3 67.8%
B4 5.5%
B1 3.6%
B2 4.1%
B3 76.8%
B4 15.4%
B1 3.1%
B2 5.6%
B3 88.6%
B4 2.7%
B1 2.6%
B2 5.8%
B3 79.8%
B4 11.8%
B1 18.5%
B2 52.0%
B3 26.7%
B4 2.8%
B1 60.5%
B2 34.2%
B3 4.7%
B4 0.6%
B1 8.3%
B2 11.8%
B3 60.1%
B4 19.7%
PI
Annexin V-FITC

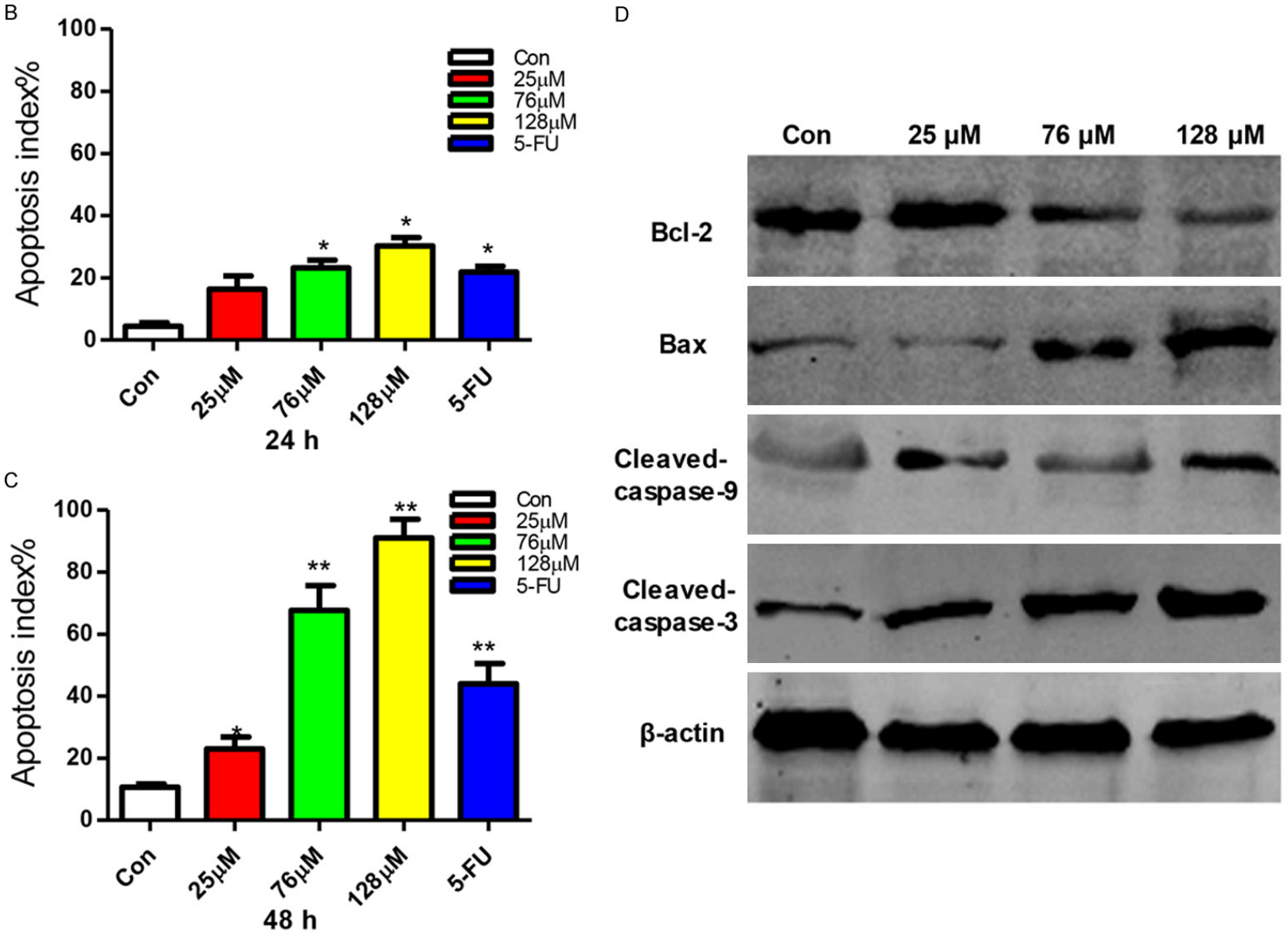

Figure 3. Compound **4** treatment induced apoptosis in Bel-7404 cells. Apoptosis value using FCM or western blot analysis was examined. A. Annexin V-FITC staining of cells were observed in the cells cultured with compound **4** for 24 h and 48 h. B, C. The percentage of apoptosis were showed as mean ± S.D. (n=2), $*P < 0.05$, $**P < 0.01$, vs control. D. Western blotting analysis of Bax, Bcl-2, caspase-9 and caspase-3 protein expression, β-actin was used as a control.

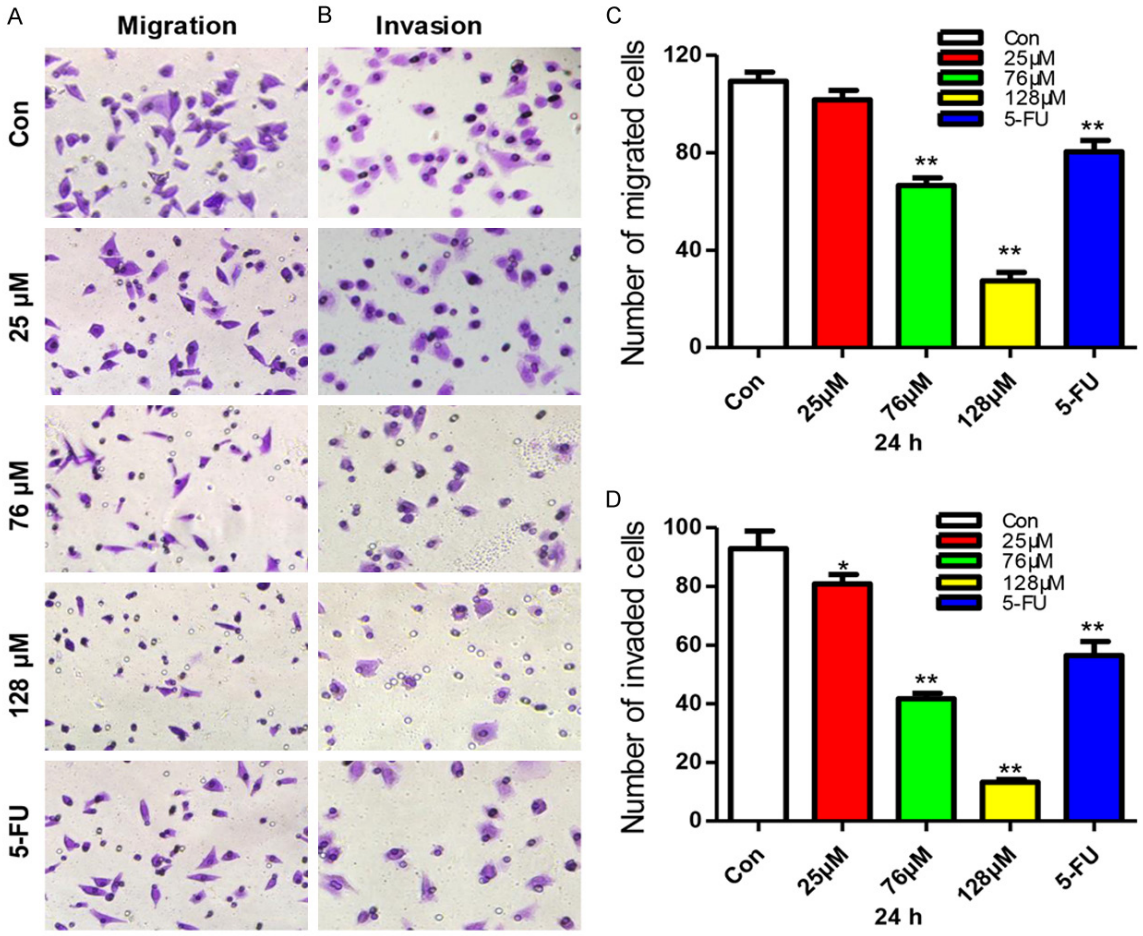

Figure 4. Compound **4** obstructed migration and invasion in Bel-7404 cells. The Bel-7404 cells treated with compound **4** (25 μM, 76 μM and 128 μM) and 5-FU for 48 h using transwell assay, respectively. (A, B) The cell migration and invasion were detected by uncoated (A) and coated (B) transwell chambers assay. (C, D) Quantitative results were illustrated for the cell migration (C) and invasion (D). **P* < 0.05; ***P* < 0.01 vs control.

observed after treatment with compound **4**. As shown in **Figure 5**, Bel-7404 cells in the control group showed a complete cellular ultrastructure: the membrane was integrity, and mitochondria and endoplasmic reticulum could be clearly observed in the cytoplasm. After treatment with compound **4** for 48 h, the cells were round and floated, and the connection between cells became loose. Distinct cytoplasmic shrinkage, membrane blebbing, formation of apoptotic bodies was clearly observed (**Figure 5**). Notably, the extent was much more obvious than that of 5-FU treatment.

*Compound **4** induces ROS production*

ROS induction centers the mechanism for chemotherapy in cancer. FCM and fluorescence microscope were used to test the levels of ROS that were induced by compound **4** exposure. As shown in **Figure 6A**, the intracellular ROS levels in Bel-7404 cells showed a definite increase after various concentrations of compound **4** for treatment 48 h ($p < 0.05$), compared with the control. Pretreatment of Bel-7404 cells for 4 h with the ROS scavenger NAC (10 mM) prior to compound **4** exposure significantly decreased cellular ROS levels (**Figure 6B**). Co-treatment of Bel-7404 cells with 10 mM NAC and different concentrations of compound **4** for 48 h remarkably alleviated cell growth inhibition induced by compound **4** (**Figure 6C**). The results revealed that oxidant damage might key to the apoptotic effects induced by compound **4** in Bel-7404 cells.

*Antitumor activity of compound **4** in vivo*

To confirm the critical role of compound **4** antitumor effect *in vivo*, we established mouse

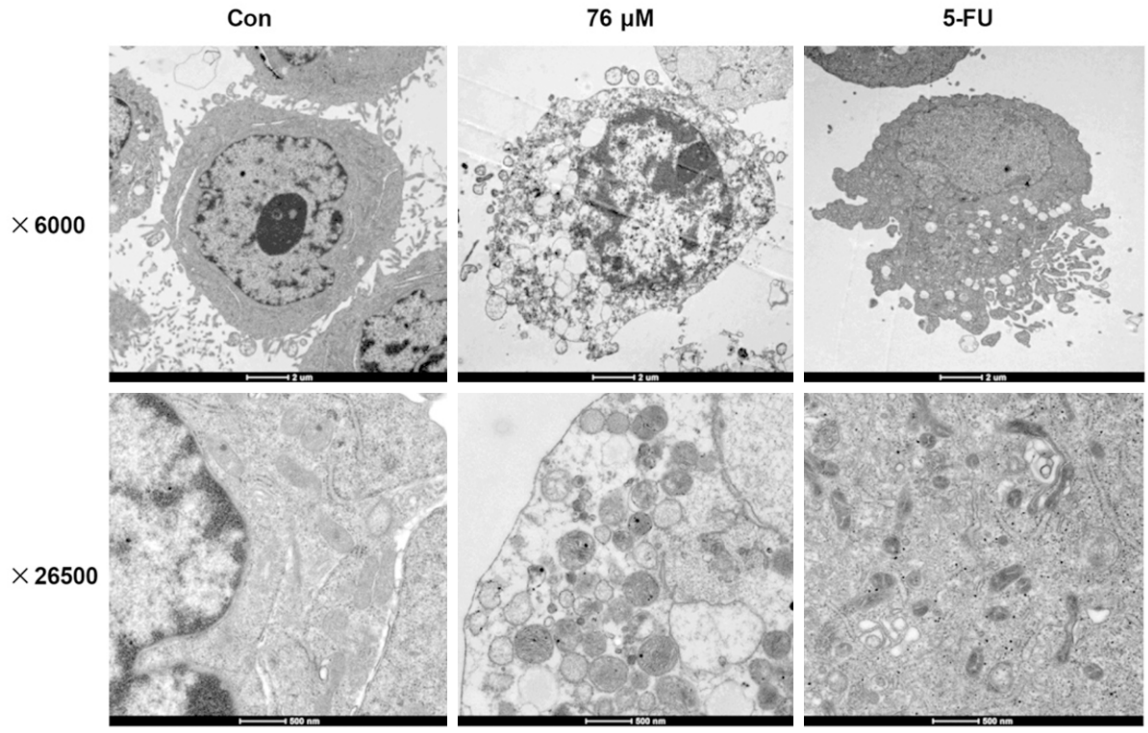

Figure 5. Morphological changes of cells observed by TEM (picture magnification × 6000, × 26500). Cells were treated with the control, compound **4** (76 μM) and 5-FU.

xenograft model bearing inoculated Bel-7404 cells. Compound **4** dose dependently reduced the tumor volume, with 60 mg/kg displayed significantly tumor growth inhibition (**Figure 7A**, **7B**), while moderate effects were seen in the low concentration of compound **4** group (20 mg/kg), which was similar to 5-FU (20 mg/kg). Moreover, treatment with compound **4** showed the maintenance of body weight. In contrast, there was a marked loss in body weight in the 5-FU group (**Figure 7C**). In addition, no obvious color fade and hair removal were seen in the compound 4 group. The absence of these side-effects signs indicates low or no toxic effects for compound **4** in mice.

Furthermore, the tumor tissues from each group were characterized by H&E staining. As shown in (**Figure 8**, upper panel), Bel-7404 cells in mice as control group presented typical fibroblast-like morphology and active cell proliferation, as evidenced by a high density of nuclear staining. In contrast, the density of the tumor cells was significantly reduced in the tumor tissues sections in compound **4** and 5-FU treated groups, suggesting that the tumor cell growth/proliferation in mice was markedly inhibited by test-drugs. Cell apoptosis in these tumor tissues was examined by TUNEL assay, as shown in (**Figure 8**, lower panel), consistent with the in vitro date. The positive stain of apoptotic cells was barely seen in the tissue sections of control group, while was obviously seen in test-drugs groups, particularly in those receiving high concentration group that caused cell death mostly. The 5-FU group (20 mg/kg) was associated with less cell apoptosis than an intermediate concentration of compound **4** (40 mg/kg).

Discussion

Hepatocellular carcinoma (HCC) is the most common tumors, with a mean survival rate of less than 5% [24, 25]. Tempol has been intensively studied as a unique and interesting class of anticancer agents against various tumors, including HCC [26]. In recent years, adamantyl derivatives have emerged as important functional groups in anticancer compounds because of their special space structure and tumor targeting specificity, which could effectively improve its activity and selectivity [27-29]. In previous study, we found a hybridized

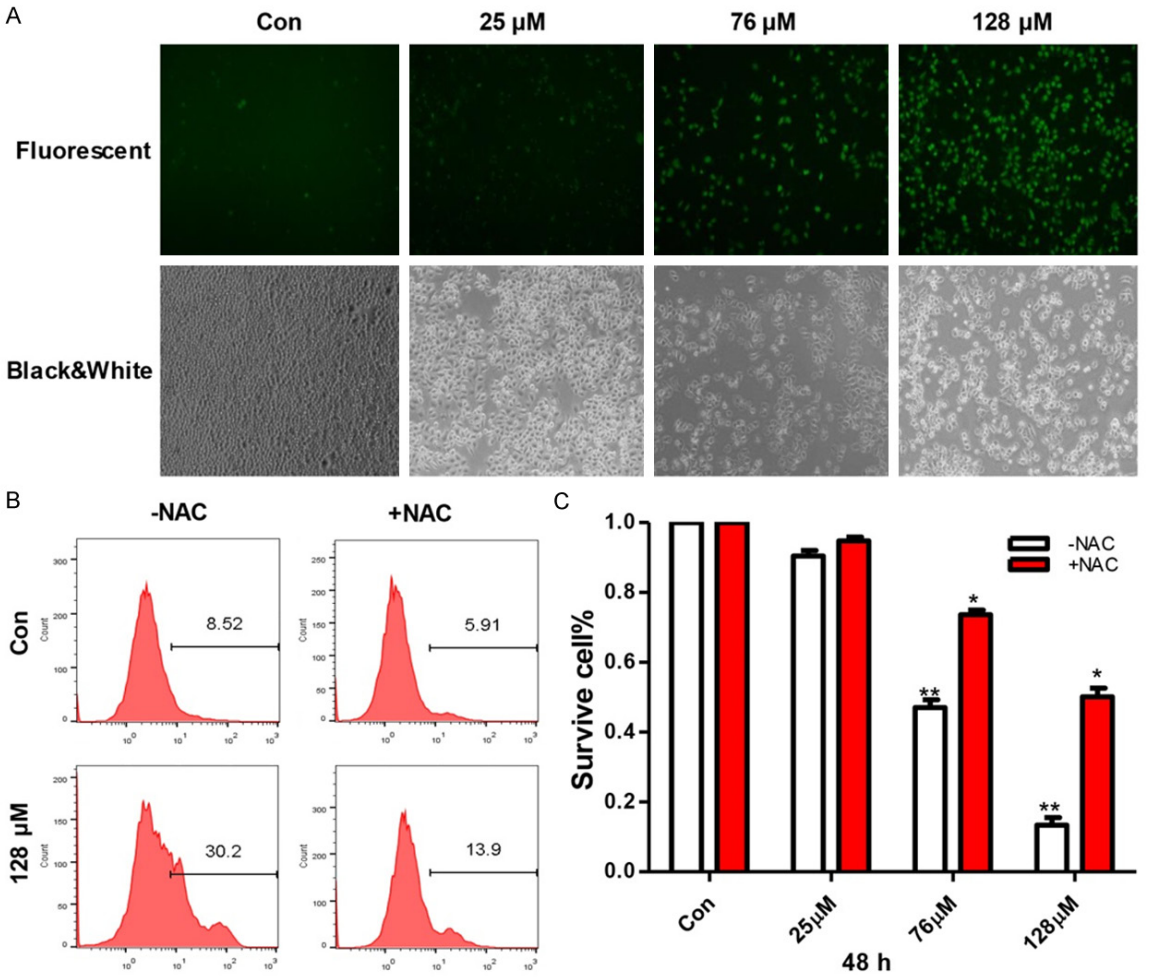

Figure 6. Effects on compound **4** induced ROS levels and cell growth inhibition in Bel-7404 cells. A. Intracellular ROS levels in Bel-7404 cells treated with compound **4** (25 μM, 76 μM and 128 μM) for 48 h using fluorescence assay, respectively. B. Effects of pretreatment for 4 h with 10 mM NAC before 128 μM compound **4** for 48 h induced ROS on Bel-7404 cells. C. The effect of co-treatment with 10 mM NAC for 48 h on cell growth inhibition in Bel-7404 cells. Values are expressed as means ± S.D (n=3). Symbols (*, **) indicate significant difference ($P < 0.05$, $P < 0.01$) to the corresponding control, respectively.

compound composed of both active pharmacophores of adamantyl moiety and Tempol, which displayed strong inhibitory activity against HCC [20]. To develop new anticancer agents, a novel adamantyl nitroxide derivative **4** was synthesized. Our current observations indicated that compound **4** did exhibit significant inhibition of proliferation and induction of apoptosis on Bel-7404 cells *in vitro* and *in vivo*.

In the present study, the cell growth inhibition and cytotoxicity assays showed that compound **4** had remarked anticancer activity on Bel-7404 cells in a dose-dependent manner (IC_{50}=68.1 μM) compared to positive control of Temopl (IC_{50}=3104.3 μM) and 5-FU (IC_{50}=607.7 μM). Additionally, there was a limited cytotoxic effect in L-02 normal cells even after high concentration and long time compound **4** exposure. Mice models bearing inoculated Bel-7404 cells were established to investigate the anticancer effect and toxicity of compound **4** *in vivo*. Compared with control group, the significant suppression of tumor growth was observed in mice treated with compound **4** without increasing tissue toxicity. After the treatment of 60 mg/kg compound **4**, the inhibitory rate of tumor weight was as high as 78.87%, while the mice have no representation of body weight loss and faded color. Based on the above observations, we then focused on evaluating the mechanism of tumor growth inhibition by compound **4**.

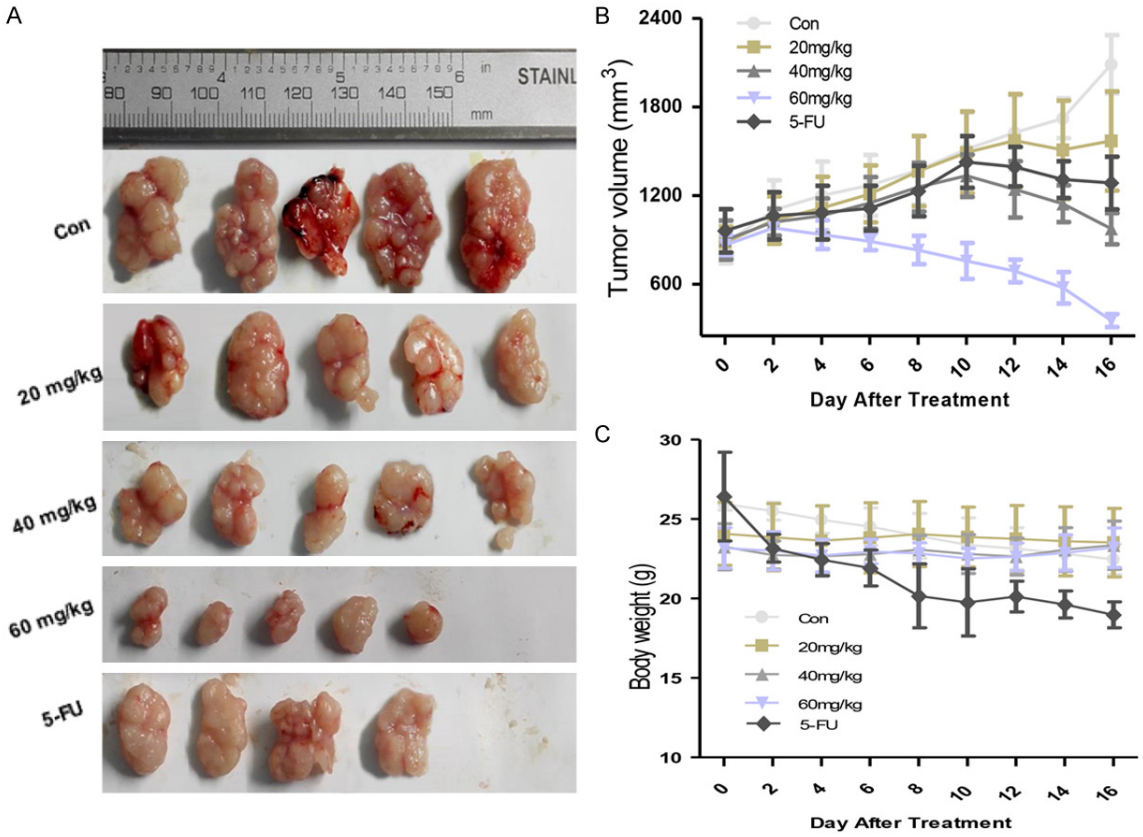

Figure 7. Suppression of Bel-7404 cells growth in mice. A. Gross tumors removed from animals after 14 days treatment. B. The tumor size was measured each two days and the volume was calculated by 0.5 × length × width^2. C. The body weight of mice in different group. Data represent the mean ± S.D. (n=5).

Cell cycle arrest is an essential mechanism for eliminating cancer cells [30]. Our study here has observed that compound **4** inhibited the proliferation via G2/M phase arrest. Besides cell cycle arrest, FCM assay also displayed that compound **4** had an apparent induction of apoptosis in Bel-7404 cells in a time- and dose-dependent manner.

Mitochondrial damage is one of the main ways of cell apoptosis, which is a hot spot in the research of apoptosis. Reactive oxygen species (ROS), which are predominantly produced in the mitochondria, play a key role in the apoptotic pathway [31, 32]. ROS, if excessive, may damage a series of cellular components, such as mitochondria, leading to the release of apoptosis-inducing factors that activate caspase cascades and induce the apoptosis of the cells [33]. The present results are highly consistent with these views. After treatment with compound **4** for 48 h, the mitochondrial swelling and deformation was clearly observed, and there were a large number of apoptosis bodies in the cell membrane. At the same time, we found that the level of intracellular ROS levels in Bel-7404 cells was significantly increased by compound **4**. Hence it would be highly speculated that compound **4** could easily break antioxidant firewall in Bel-7404 cells, which in turn remarkably alleviated cell growth inhibition and increased the cell survival rate. These results revealed that compound-induced ROS accumulation was involved in Bel-7404 cells apoptosis.

Besides ROS, the anti-apoptotic protein Bcl-2 and pro-apoptotic protein Bax, which regulate the permeability of the mitochondrial membrane and induce the activation of caspase, are also important for the process of drug-induced apoptosis [34]. Mitochondrial damage facilitates the release of cytochrome C from mitochondria into the cytoplasm and the formation of apoptotic bodies to activate caspase-9 and caspase-3, which leads to activation of the cas-

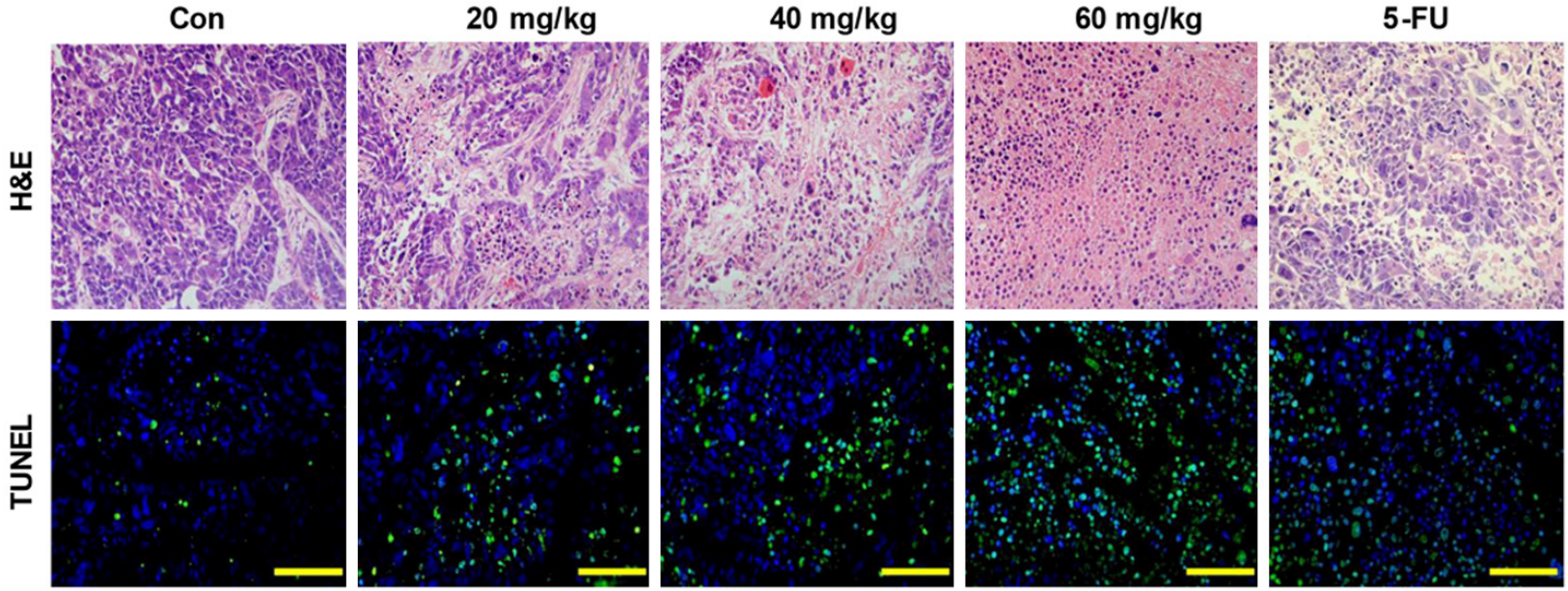

Figure 8. Histological analyses of antitumor activities of compound **4**. After paraformaldehyde fixing and paraffin embedding, the sections were stained with H&E for histological examination (upper panel). Data are a typical microscopic imaging of tumor tissue sections under original magnification of × 200. H&E Nuclei: blue, cytoplasm: pink. Apoptotic cells in tissues sections were detected by TUNEL assay (lower panel). Data are a typical fluorescent microscopic imaging of tumor tissue sections under original magnification of × 200. Nuclei: blue, apoptosis cells: green.

pase cascades and mitochondria-mediated apoptosis [35]. We analyzed the expression of Bcl-2, Bax, caspase-9 and caspase-3 in Bel-7404 cells treated with compound **4** at different concentrations. Our results showed that compound **4** clearly decreased expression levels of Bcl-2 and increased expression levels of Bax, caspase-9 and caspase-3 in a dose-dependent manner. These data further suggested that compound **4** induced apoptosis of Bel-7404 cells by regulating mitochondrial apoptosis pathway. Our data *in vitro* and *in vivo* indicated that the antitumor effect of compound **4** might have a relationship not only with the triggered oxidative stress but also with the mitochondria damage induced by other mechanisms.

In conclusion, the adamantyl nitroxide derivative **4**, which was composed of both active pharmacophores of adamantyl moiety and Tempol, showed strong cancer inhibitory activities against Bel-7404 cells *in vitro* and *in vivo*. Mechanistically, compound **4** acted via reduction of cell proliferation, migration, invasion, and inducing apoptosis. These activities of compound **4** were associated with mitochondrial apoptosis pathway and oxidative stress. This study provides evidence that compound **4**, as an adamantyl nitroxide derivative, is a promising candidate for treatment of liver cancer, which still requires further investigation.

Acknowledgements

This work was financially supported by National Natural Science Foundation of China, No. 81302627, 81302695 and 81502903.

Disclosure of conflict of interest

None.

Address correspondence to: Drs. Xiao-He Zhu and Ai-Dong Wen, Department of Pharmacy, Xijing Hospital, Fourth Military Medical University, Xi'an, Shaanxi 710032, China. Tel: +86-029-84775475; Fax: +86-029-84775475; E-mail: xiaohezhu@hotmail.com (XHZ); adwen-2004@hotmail.com (ADW); Dr. Guo-Dong Yang, State Key Laboratory of Cancer Biology, Department of Biochemistry and Molecular Biology, Fourth Military Medical University, Xi'an, Shaanxi 710032, China. Tel: +86-029-84775475; Fax: +86-029-84775475; E-mail: yanggd@fmmu.edu.cn

References

[1] Jemal A, Bray F, Center MM, Ferlay J, Ward E and Forman D. Global cancer statistics. CA Cancer J Clin 2011; 61: 69-90.

[2] Oliveri RS, Wetterslev J and Gluud C. Hepatocellular carcinoma. Lancet 2012; 380: 470.

[3] Tejeda-Maldonado J, Garcia-Juarez I, Aguirre-Valadez J, Gonzalez-Aguirre A, Vilatoba-Chapa M, Armengol-Alonso A, Escobar-Penagos F, Torre A, Sanchez-Avila JF and Carrillo-Perez DL. Diagnosis and treatment of hepatocellular carcinoma: An update. World J Hepatol 2015; 7: 362-376.

[4] Zhao L, Li H, Shi Y, Wang G, Liu L, Su C and Su R. Nanoparticles inhibit cancer cell invasion and enhance antitumor efficiency by targeted drug delivery via cell surface-related GRP78. Int J Nanomedicine 2015; 10: 245-256.

[5] Maluccio M and Covey A. Recent progress in understanding, diagnosing, and treating hepatocellular carcinoma. CA Cancer J Clin 2012; 62: 394-399.

[6] Wang H, Jia Y, Gao P, Cheng Y, Cheng M, Lu C, Zhou S and Sun X. Synthesis, radioprotective activity and pharmacokinetics characteristic of a new stable nitronyl nitroxyl radical-NIT2011. Biochimie 2013; 95: 1574-1581.

[7] Vorobjeva NV and Pinegin BV. Effects of the antioxidants Trolox, Tiron and Tempol on neutrophil extracellular trap formation. Immunobiology 2016; 221: 208-219.

[8] Patel K, Chen Y, Dennehy K, Blau J, Connors S, Mendonca M, Tarpey M, Krishna M, Mitchell JB, Welch WJ and Wilcox CS. Acute antihypertensive action of nitroxides in the spontaneously hypertensive rat. Am J Physiol Regul Integr Comp Physiol 2006; 290: R37-43.

[9] Zhao B, Pan Y, Wang Z, Tan Y and Song X. Intrathecal Administration of Tempol Reduces Chronic Constriction Injury-Induced Neuropathic Pain in Rats by Increasing SOD Activity and Inhibiting NGF Expression. Cell Mol Neurobiol 2016; 36: 893-906.

[10] Liu YQ, Li XJ, Zhao CY, Nan X, Tian J, Morris-Natschke SL, Zhang ZJ, Yang XM, Yang L, Li LH, Zhou XW and Lee KH. Synthesis and mechanistic studies of novel spin-labeled combretastatin derivatives as potential antineoplastic agents. Bioorg Med Chem 2013; 21: 1248-1256.

[11] Mitchell JB, DeGraff W, Kaufman D, Krishna MC, Samuni A, Finkelstein E, Ahn MS, Hahn SM, Gamson J and Russo A. Inhibition of oxygen-dependent radiation-induced damage by the nitroxide superoxide dismutase mimic, tempol. Arch Biochem Biophys 1991; 289: 62-70.

[12] Zhao XB, Wu D, Wang MJ, Goto M, Morris-Natschke SL, Liu YQ, Wu XB, Song ZL, Zhu GX and Lee KH. Design and synthesis of novel spin-labeled camptothecin derivatives as potent cytotoxic agents. Bioorg Med Chem 2014; 22: 6453-6458.

[13] Gadjeva VG. Two spin labeled triazenes: relationship between biochemical and biological activities. Int J Pharm 2002; 247: 39-45.

[14] Gish DT, Kelly RC, Camiener GW and Wechter WJ. Nucleic acids. 11. Synthesis of 5'-esters of 1-beta-D-arabinofuranosylcytosine possessing antileukemic and immunosuppressive activity. J Med Chem 1971; 14: 1159-1162.

[15] Al-Abdullah ES, Al-Tuwaijri HM, Hassan HM, Al-Alshaikh MA, Habib EE and El-Emam AA. Synthesis, Antimicrobial and Hypoglycemic Activities of Novel N-(1-Adamantyl)carbothioamide Derivatives. Molecules 2015; 20: 8125-8143.

[16] Liu J, Obando D, Liao V, Lifa T and Codd R. The many faces of the adamantyl group in drug design. Eur J Med Chem 2011; 46: 1949-1963.

[17] Lee K, Lee JH, Boovanahalli SK, Jin Y, Lee M, Jin X, Kim JH, Hong YS and Lee JJ. (Aryloxyacetylamino) benzoic acid analogues: A new class of hypoxia-inducible factor-1 inhibitors. J Med Chem 2007; 50: 1675-1684.

[18] Dawson MI, Xia Z, Liu G, Ye M, Fontana JA, Farhana L, Patel BB, Arumugarajah S, Bhuiyan M, Zhang XK, Han YH, Stallcup WB, Fukushi J, Mustelin T, Tautz L, Su Y, Harris DL, Waleh N, Hobbs PD, Jong L, Chao WR, Schiff LJ and Sani BP. An adamantyl-substituted retinoid-derived molecule that inhibits cancer cell growth and angiogenesis by inducing apoptosis and binds to small heterodimer partner nuclear receptor: effects of modifying its carboxylate group on apoptosis, proliferation, and protein-tyrosine phosphatase activity. J Med Chem 2007; 50: 2622-2639.

[19] Nepali K, Sharma S, Sharma M, Bedi PM and Dhar KL. Rational approaches, design strategies, structure activity relationship and mechanistic insights for anticancer hybrids. Eur J Med Chem 2014; 77: 422-487.

[20] Zhu XH, Sun J, Wang S, Bu W, Yao MN, Gao K, Song Y, Zhao JY, Lu CT, Zhang EH, Yang ZF and Wen AD. Synthesis, crystal structure, superoxide scavenging activity, anticancer and docking studies of novel adamantyl nitroxide derivatives. J Mol Struct 2016; 1108: 611-617.

[21] Guo J, Zhang Y, Zhang J, Liang J, Zeng L and Guo G. Anticancer effect of tert-butyl-2(4,5-dihydrogen-4,4,5,5-tetramethyl-3-0-1H-imidazole-3-cationic-1-oxy l-2)-pyrrolidine-1-carboxylic ester on human hepatoma HepG2 cell line. Chem Biol Interact 2012; 199: 38-48.

[22] Hu W, Fu J, Lu SX, Liu LL, Luo RZ, Yun JP and Zhang CZ. Decrease of Bcl-xL/Bcl-2-associated death promoter in hepatocellular carcinoma indicates poor prognosis. Am J Cancer Res 2015; 5: 1805-1813.

[23] Eaton PE, Nordari N, Tsanaktsidis J and Upadhyaya SP. Barton Decarboxylation Of Cubane-1,4-Dicarboxylic Acid - Optimized Procedures for Cubanecarboxylic Acid And Cubane. Synthesis-Stuttgart 1995; 501-502.

[24] Alves RC, Alves D, Guz B, Matos C, Viana M, Harriz M, Terrabuio D, Kondo M, Gampel O and Polletti P. Advanced hepatocellular carcinoma. Review of targeted molecular drugs. Ann Hepatol 2011; 10: 21-27.

[25] Waly Raphael S, Yangde Z and Yuxiang C. Hepatocellular carcinoma: focus on different aspects of management. ISRN Oncol 2012; 2012: 421673.

[26] Soule BP, Hyodo F, Matsumoto K, Simone NL, Cook JA, Krishna MC and Mitchell JB. The chemistry and biology of nitroxide compounds. Free Radic Biol Med 2007; 42: 1632-1650.

[27] Altucci L, Leibowitz MD, Ogilvie KM, de Lera AR and Gronemeyer H. RAR and RXR modulation in cancer and metabolic disease. Nat Rev Drug Discov 2007; 6: 793-810.

[28] Dawson MI, Harris DL, Liu G, Hobbs PD, Lange CW, Jong L, Bruey-Sedano N, James SY, Zhang XK, Peterson VJ, Leid M, Farhana L, Rishi AK and Fontana JA. Antagonist analogue of 6-[3'-(1-adamantyl)-4'-hydroxyphenyl]-2-naphthalenecarboxylic acid (AHPN) family of apoptosis inducers that effectively blocks AHPN-induced apoptosis but not cell-cycle arrest. J Med Chem 2004; 47: 3518-3536.

[29] Kaur G, Narayanan VL, Risbood PA, Hollingshead MG, Stinson SF, Varma RK and Sausville EA. Synthesis, structure-activity relationship, and p210(bcr-abl) protein tyrosine kinase activity of novel AG 957 analogs. Bioorg Med Chem 2005; 13: 1749-1761.

[30] Buolamwini JK. Cell cycle molecular targets in novel anticancer drug discovery. Curr Pharm Des 2000; 6: 379-392.

[31] Deavall DG, Martin EA, Horner JM and Roberts R. Drug-induced oxidative stress and toxicity. J Toxicol 2012; 2012: 645460.

[32] Trachootham D, Alexandre J and Huang P. Targeting cancer cells by ROS-mediated mechanisms: a radical therapeutic approach? Nat Rev Drug Discov 2009; 8: 579-591.

[33] Zamzami N, Marchetti P, Castedo M, Decaudin D, Macho A, Hirsch T, Susin SA, Petit PX, Mignotte B and Kroemer G. Sequential reduction of mitochondrial transmembrane potential and generation of reactive oxygen species in early programmed cell death. J Exp Med 1995; 182: 367-377.

[34] Ji YB, Qu ZY and Zou X. Juglone-induced apoptosis in human gastric cancer SGC-7901 cells via the mitochondrial pathway. Exp Toxicol Pathol 2011; 63: 69-78.
[35] Wu M, Zhang H, Hu J, Weng Z, Li C, Li H, Zhao Y, Mei X, Ren F and Li L. Isoalantolactone inhibits UM-SCC-10A cell growth via cell cycle arrest and apoptosis induction. PLoS One 2013; 8: e76000.